SELF-IGNITION OF HYDROGEN JET FIRES BY ELECTROSTATIC DISCHARGE INDUCED BY ENTRAINED PARTICULATES

Merilo, E.G.[1], Groethe, M.A.[1], Adamo, R.C.[1], Schefer, R.W.[2], Houf, W.G.[2] and Dedrick, D.E.[2]
[1] SRI International, Menlo Park, CA 94025, USA, erik.merilo@sri.com
[2] Sandia National Laboratories, Livermore, CA 94551-0969, USA, will@sandia.gov

ABSTRACT

The potential for particulates entrained in hydrogen releases to generate electrostatic charge and induce electrostatic discharge ignitions was investigated. A series of tests were performed in which hydrogen was released through a 3.75-mm-diameter orifice from an initial pressure of 140 bar. Electrostatic field sensors were used to characterize the electrification of known quantities of iron oxide particulates deliberately entrained in the release. The ignition experiments focused on using charged particulates to induce spark discharges from isolated conductors and corona discharges. A total of 12 ignition events were observed. The results show that electrification of entrained particulates is a viable self-ignition mechanism of hydrogen releases.

1.0 INTRODUCTION

Numerous hydrogen release events have resulted in the ignition of the hydrogen jet with no clear ignition source. This phenomenon is called self-ignition, spontaneous ignition, or auto ignition. Astbury and Hawksworth [1] performed a review of spontaneous ignition incidents and of postulated mechanisms. In their review of hydrogen release incidents, the source of ignition was not identified in 86.3% of cases. They then postulated five potential mechanisms that could cause self-ignition of a hydrogen release: (1) Reverse Joule-Thomson effect; (2) Electrostatic ignition; (3) Diffusion ignition; (4) Sudden adiabatic compression; and (5) Hot surface ignition. Astbury and Hawksworth concluded that the reverse Joule-Thomson effect, sudden adiabatic compression, and hot surface ignition were unlikely to be ignition sources in the majority of hydrogen incidents. Of the postulated mechanisms, diffusion ignition has been the primary focus of research [2-4].

While diffusion ignition has been shown to be a viable self-ignition mechanism, there have been several hydrogen ignition incidents that cannot be explained by this mechanism [1, 5-8]. For these ignition events, an electrostatic discharge ignition may provide a viable ignition mechanism. However, there has been a very limited amount of research to investigate electrostatic charge generation and discharge as an ignition source of hydrogen releases. Imamura et al. [9] performed experiments on the electrification of iron oxide particles in a ventilation duct outlet and showed that charge was accumulated on the iron oxide particles and that the total energy accumulated on a wire gauze placed in the release was greater than the minimum ignition energy of hydrogen. Royle et al. [10] attempted to ignite a hydrogen release by inducing a corona discharge on grounded wire probes using plastic powder and iron oxide particles. In this study, no ignition events were induced by charge particles.

The ignition of a flammable mixture is not caused by charge buildup alone. A number of stages must occur for the charge to ignite a mixture [11-12]. These stages are:

1. Charge separation (generation of electrostatic charge)
2. Charge accumulation
3. Charge removal
    3.1 Charge removal by dissipation → no ignition
    3.2 Charge removal by electrostatic discharge → possible ignition
4. Flammable mixture
5. Discharge energy greater than the minimum ignition energy

It is possible for a release from a pressurized hydrogen system to produce the stages necessary for electrostatic discharge ignition to occur. In a hydrogen release, there is a potential for the generation and accumulation of significant static charge which, combined with an appropriate discharge geometry in the presence of a flammable mixture, could lead to ignition by electrostatic discharge. Charge separation can be produced by a number of different mechanisms. Rapidly moving pure gases containing no particulates have been shown to generate little or no electrostatic charge [13-14]. If the moving gas is contaminated by a small amount of solid particulates or liquid droplets, there is potential for electrostatic charge to be generated. The movement of particles over a surface is a common source of static electricity [15-16] with the most common mechanism being triboelectric charging. In natural gas pipelines, it is common to find magnetite-containing iron (II) oxide and iron (III) oxide, with bimodal particle distribution with peaks at 30 μm and 0.3 μm [17]. In pressurized hydrogen systems, it is also possible for these types of particles and other solid particulates to be present [18].

Charge accumulation occurs when the charge-generation rate exceeds the rate of charge dissipation [19]. The most common reason for a conductor to be charged to a high potential is the lack of a path to ground [20]. When particles are charged while traveling through a pipe, charge can accumulate on the particles due to their isolation from ground. The charged particles can also cause charge accumulation on objects both inside the release and in close proximity to it. Objects in or near the release can be charged by induction, while objects in the release can also be charged by impact charging. Charge accumulation is a paramount concern for insulating surfaces, low-conductivity particles, and ungrounded conductors. A vast majority of electrostatic ignition accidents can be attributed to the presence of isolated conductors [20].

A discharge can occur when the charge on an object accumulates to a level at which the electric field produced exceeds the dielectric strength of the surrounding atmosphere. If the charged particles interact with a suitable grounding condition and geometric configuration, a discharge can be produced that is energetic enough to result in ignition of the surrounding flammable gas mixture. For flammable gas mixtures, there are four types of electrostatic discharge mechanisms that can lead to ignition [14]: (1) spark discharge between isolated conductors; (2) brush discharges; (3) corona discharges; and (4) propagating brush discharges. A spark discharge can occur when isolated conductors in close proximity are charged to different electrostatic potentials. A brush discharge can occur when a grounded conductive electrode, with a radius of curvature more than a few millimeters, is brought into an electric field of sufficient strength [14]. The conditions required for a corona discharge are similar to those that create a brush discharge. Corona discharges are generated in areas of high field strength, which can develop around sharp points with a radius of curvature less than 3 to 5 mm [18-20]. Propagating brush discharges can form when two layers of an object are charged to opposite polarities.

When a discharge occurs, some or all of the stored energy may be released. If the energy of the discharge is greater than the minimum ignition energy of the surrounding flammable gas mixture, then ignition can occur. Due to its ignition sensitivity, hydrogen-air mixtures tend to be more susceptible to electrostatic ignition than other reacting jet releases. The wide flammability range of hydrogen means that a release can produce a sizeable flammable extent. For a near-stoichiometric mixture, the minimum ignition energy of hydrogen and air is 0.017 mJ [21]. The spark ignition energy required for ignition is only about 6 mJ [21] at the upper and lower flammability limits.

2.0 EXPERIMENTAL SETUP

2.1 Hydrogen-Release Facility

A pressurized hydrogen-release facility was used to characterize the electrification of entrained iron oxide particulates and to investigate possible ignition mechanisms. The hydrogen release facility consists of six components: (1) the pressurized hydrogen source; (2) high-pressure lines; (3) a stagnation chamber; (4) a release valve; (5) a particle-entrainment tube; and (6) a nozzle. Fig. 1 shows a schematic of the flow-delivery system.

The pressurized hydrogen was stored in a modified tank consisting of a standard 1A bottle, with a volume of 43.8 liters. The modified hydrogen tank was filled to about 140 bar with hydrogen using a commercial "six-pack." The pressure in the modified tank was measured with a Sensotec TJE differential pressure transducer. High-pressure stainless steel lines with Swagelok fittings were used to connect the modified hydrogen tank to the stagnation chamber. The stagnation chamber was located just upstream of the release valve and particle-entrainment tube. This chamber was used in previous studies with this release facility [22]. It was designed so that the flow inside was at a low Mach number, with internal dimensions of 26.1 cm in length and a diameter of 15.3 cm. The pressure inside the stagnation chamber was measured with an Omega MMSG2.5KV10P4C1T3A5 piezoresistive pressure transducer, and the temperature was measured with a type-T thermocouple.

The release valve used in this test series was a Tescom VG-C6CBVG9H9 air-operated valve. This valve has an actuation time of less than 75 ms. The total volume of the release facility upstream of the valve was 0.0487 m^3. Once the valve was opened, the hydrogen was released into the particle-entrainment tube, which was filled with air at ambient pressure. A T-connector located on the upstream end of the tube allows a given mass of particles to be placed inside the tube and entrained in the hydrogen release. The particle-entrainment tube was a steel pipe with an inside diameter of 25.4 mm and a length of 3.05 m. The 3.175-mm stainless steel nozzle was attached to the downstream side of the particle-entrainment tube with a Swagelok fitting.

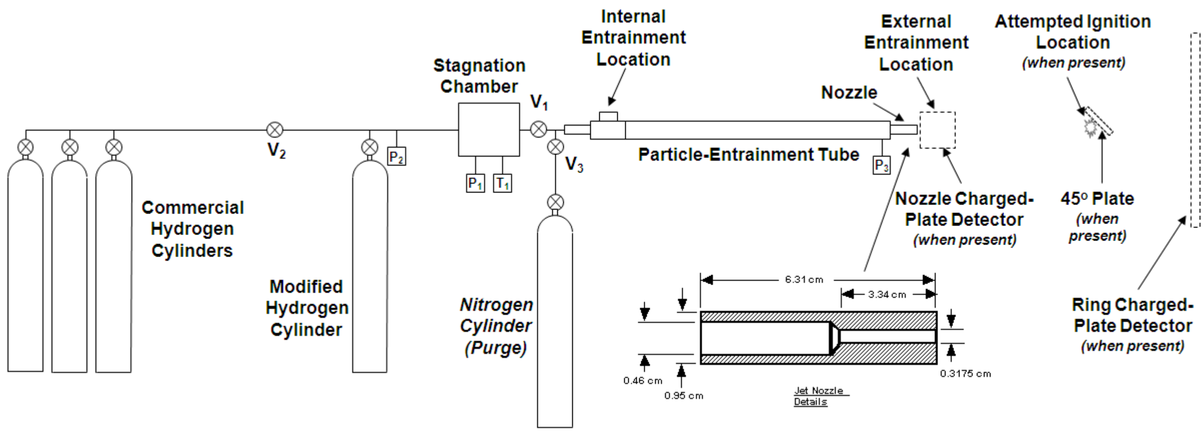

Figure 1. Schematic of experimental flow-delivery system.

2.2 Instrumentation

Ignition location and flame propagation were monitored using a combination of standard, infrared, and high-speed video. The charge accumulated on iron oxide particles entrained in the hydrogen jet was measured using a two-channel ETS Model 624 Static Level Monitoring System. Two sealed non-contacting chopper-stabilized sensors were used to measure the charge induced onto two separate isolated detector plates. The sensor assemblies were located outside the hydrogen jet. Charged-plate detectors were used in conjunction with the monitoring system. A 40-kV-rated silicon cable was used to transfer the charge from the charged-plate detector to a second plate monitored by an electrostatic sensor.

Two types of charged-plate detectors were used in the charge characterization tests: a nozzle charged-plate detector and a ring charged-plate detector. The detectors can be charged by induction, when particles pass through the center, or by contact, when a particle strikes the detector and imparts a charge. Fig. 2 shows the charged-plate detectors along with the origin used to reference the sensor positions, located just in front of the nozzle. The external particle-entrainment tests used only the ring charged-plate detector. The ring charged-plate detector, located on an axis with the nozzle 1.52 m away, was designed to detect the static charge generated by the conical spray from the nozzle. Two different sizes (76 mm and 127 mm) of nozzle charged-plate detectors were used during the tests.

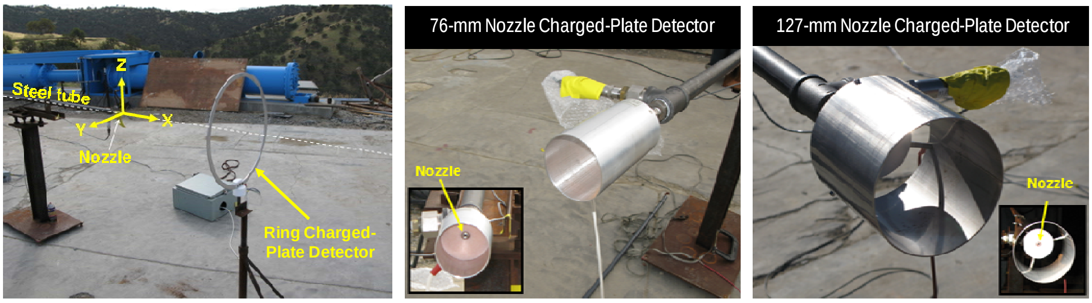

Figure 2. Charged-plate detectors and reference origin located at the release nozzle.

At the beginning of each test series the static level monitoring system was calibrated by placing a known voltage on each of the detectors, using a Spellman SL30 High Voltage Power Supply. During a test, the charged-plate detectors can build up a significant charge and may remain charged even after the test is completed. After every test, the charged-plate detectors were discharged with a grounding wire, and the static level monitoring system was zeroed prior to taking a measurement.

2.3 Iron Oxide Samples

Four iron oxide samples were tested in this study: three iron (III) oxide samples (Samples A through C); and one iron (II) oxide sample (Sample D). Electron micrographs of each sample were collected, using secondary electron imaging (SEI) and backscattered electron imaging (BEI). Selected SEI images for Samples A through D are shown in Fig. 3. All four samples were tested in the external particle-entrainment tests. The particles that produced the highest charge were then used in the internal entrainment test. Sample B contained that largest iron (III) oxide particles, with a maximum particle diameter of 140 µm and average particle diameter of 17 µm. Samples A, C, and D had average particle diameters of 15 µm, 9 µm, and 14 µm, respectively.

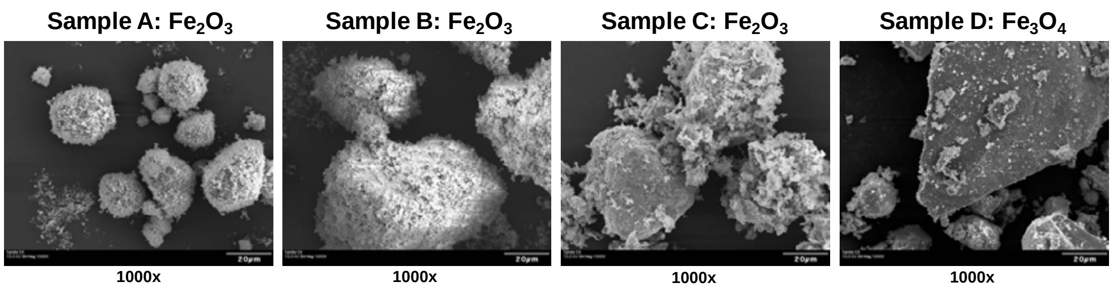

Figure 3. Secondary electron imaging for iron oxide samples A through D.

2.4 Approach

The objective of this research was to determine whether a static charge accumulation on iron oxide particles, entrained in a hydrogen jet release, could lead to a spark discharge ignition or a corona discharge ignition. Three different types of experiments were performed: (1) ignition experiments with energy input from an external power supply; (2) entrained particulate electrification characterization experiments; and (3) ignition by entrained electrified particulates experiments.

Ignition experiments, with energy input from an external power supply, were conducted to show that the release could be ignited at the selected ignition location. The location was chosen based on previous work performed with the release facility [22]. All subsequent tests used the same location to attempt ignition. The discharge mechanisms investigated were spark discharge between isolated conductors and corona discharge.

Entrained particulate electrification characterization experiments were performed to obtain a baseline for the release facility and to identify which particles generated the highest electrostatic charge. Electric field sensors were used to characterize the release. The experiments were divided into the following categories: (1) baseline experiments with no particles; (2) external particle-entrainment experiments; and (3) internal particle-entrainment experiments. The external particle-entrainment experiments were used to evaluate how particulate electrification was affected by the different iron oxide particle samples. In these tests, particles were placed in a T-connecter that was attached to the release nozzle. This was done so that the internal surfaces of the release facility would not be contaminated by different types of particles. The particulates that were charged to the highest potential were then used in the internal entrainment experiments. The internal particle-entrainment experiments were performed to investigate how particulate electrification was affected by the particle-entrainment location and by the total mass of the iron oxide particles entrained in the release.

Ignition experiments by entrained electrified particulates were performed in an attempt to generate electrostatic discharges that ignited the release. The discharges investigated in these experiments were electrostatic discharges between isolated conductors and corona discharges. An ungrounded plate next to a grounded probe was used in an attempt to create an electrostatic discharge between isolated conductors. Attempts to generate a corona discharge were performed using a sharp, pointed, ungrounded plate, which could be charged to a very high potential, and grounded probes, in which the charged particles in the release were discharged to ground by a corona discharge.

3.0 RESULTS AND DISCUSSION

3.1 Ignition Tests with Energy Input from an External Power Supply

A total of seven ignition tests with energy supplied by an external power supply were conducted. One test was performed with a continuous spark-ignition module to verify that the release could be ignited at the selected ignition location by a spark discharge. The total available energy from the spark ignition module was 110 mJ. The hydrogen release in this test was ignited by the spark. The ignition location in all tests was (0.91 m, 0.14 m, 0.00 m) as referenced to the X, Y, Z origin shown in Fig. 2. This location was used for all subsequent tests.

Four tests were conducted with an alternating current (AC) corona generator connected to a copper probe. An AC corona does not represent the corona that could be induced by charged particulates. These tests were conducted to investigate the potential for any type of corona to ignite a hydrogen release. The corona voltage was varied from 10 – 18 kV. None of the tests performed with the AC corona ignited the hydrogen release.

3.2 Entrained Particulate Electrification Characterization Tests

The particulate electrification characterization tests were performed to: (1) measure a baseline for the system with no particles; (2) determine how different types and quantities of particles influence the charge generated; and (3) find a configuration that generates the highest electrostatic charge. The configuration that generated the highest electrostatic charge was then used in subsequent ignition tests. The static charge characterization tests focused on the variation of four different parameters: (1) total number of releases performed with no particles; (2) type of iron oxide particle; (3) particle-entrainment location; and (4) total mass of the iron oxide particles added.

The first set of tests measured the static charge generated during repeated releases from the release facility with no particles added. Fig. 4(a) compares the measurements made with the ring charged-plate detector for release tests with no particles. Release 1 was the first release performed after the release facility had been constructed. Since pure gases generate a negligible amount of charge [13-14], it is assumed that any charge detected in these releases can be attributed to stray particles that were initially inside the system. A significant amount of charge was generated during the first release, indicating the facility was contaminated during construction. The amount of charge generated in each test decreased significantly for subsequent releases. These tests show there is potential for the electrification of particulate matter contained in a hydrogen storage system. The data suggest that repeated releases were effective at reducing the amount of particulate matter in the system, thereby reducing the amount of charge generated.

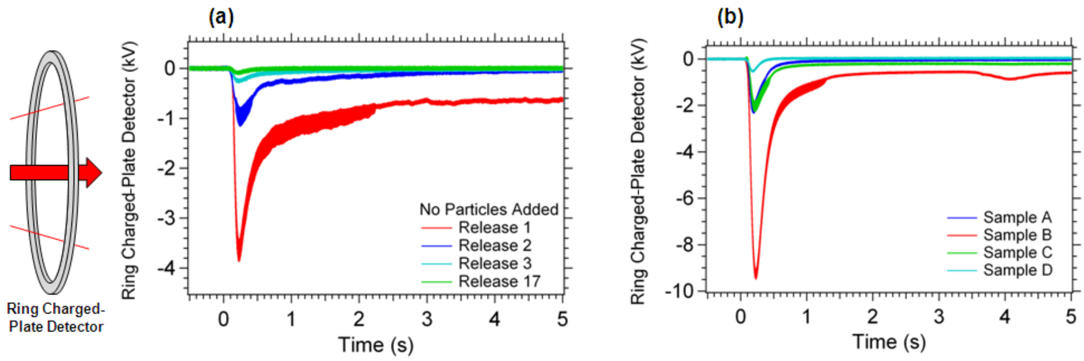

Figure 4. Electrostatic potential measurement on the ring charged-plate detector for release tests with: (a) no particles added; and (b) iron oxide samples A through D.

When charged particles flow by a charged-plate detector without colliding with it, a charge will be induced on the detector. This charge will return to zero when the particles move away from the detector. When the charged particles collide with the detector, they can deposit a charge through impact charging. This charge will stay on the plate after the particle has moved away. The data from the ring charged-plate detector show a rapid increase in charge that recedes when the particles have passed, indicating that a majority of the measured charge was induced by the particles. Only a small amount of charge was produced by particles impacting the detector.

In all the measurements taken during this study, there was significantly more scatter in the charge data measured by the 76-mm nozzle charged-plate detector than the ring charged-plate detector. This was probably due to variation in the number of particles coming into contact with the detector, rather than variation in the total charge on the particles. This led to the eventual replacement of the 76-mm nozzle charged-plate detector with the 127-mm nozzle charged-plate detector, which significantly reduced the potential for particles to collide with the detector.

The second set of tests evaluated the electrification of iron oxide samples externally entrained in the hydrogen jet. The external entrainment location is shown in Fig. 1. Fig. 4(b) shows a comparison of the static charge measurement by the ring charged-plate detector for iron oxide samples A – D. All four iron oxide particles induced a negative charge on the detector, indicating that electrons were stripped from the iron oxide particles and gave them a positive charge. Of the four samples, sample B produced the highest charge. Based on these results, sample B was selected for the internal entrainment tests.

The third set of tests was performed with particles entrained inside the release facilities' particle-entrainment tube. The internal entrainment location is shown in Fig. 1. Fig. 5(a) shows a comparison of the charge measurement on the ring charged-plate detector for tests with no particles and those with external and internal particle entrainment. More tests are required to determine repeatability; however, the plot indicates the charge on the particles increased when the particles were entrained inside the particle-entrainment tube. This was probably caused by the particles in the tube having electrons removed during collisions with the tube wall. While the charge was higher for internally entrained particles, significant charge was still produced by particles entrained outside the release facility. This could indicate that the particles from sample B had a significant initial charge that could not be dissipated to ground when the particles contacted the grounded T-connector, or that the collisions within the T-connector were sufficient to charge the particles.

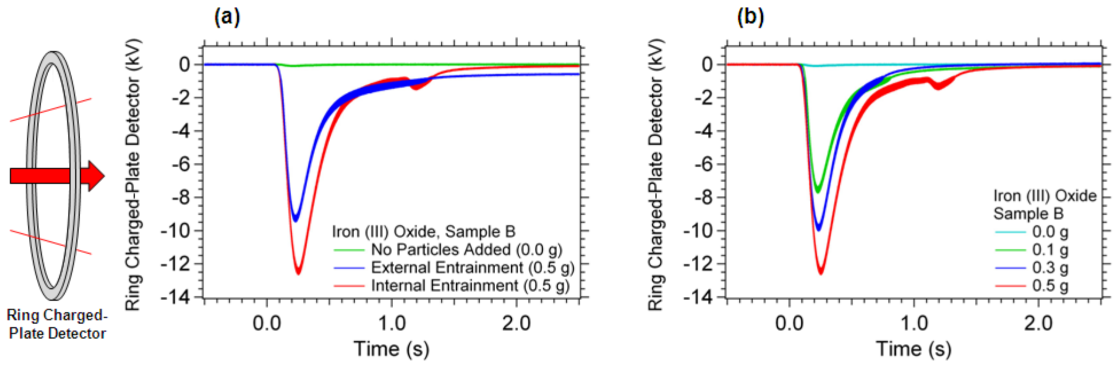

Figure 5. Electrostatic potential measurement on the ring charged-plate detector for tests with: a) no particles, external, and internal particle entrainment; and b) varying iron oxide mass.

In the fourth set of tests, the total mass of particles entrained internally was varied. Iron oxide sample B was used. Fig. 5(b) shows the charge measured on the ring detector. Over the range of mass investigated, the charge increased with increasing particle mass. The increase in charge on the detector from the “no particle” case to the case with 0.1 g was very large compared with the increases that were observed when 0.3 g and 0.5 g of iron oxide were used. This indicates that a very small quantity of particles in a pressurized hydrogen facility has the potential to produce a significant electrostatic of charge.

3.3 Self-Ignition Events

Spark Discharges Between Isolated Conductors: Ungrounded Plate/Grounded Probe

A series of ignition tests was performed with a circular ungrounded plate in close proximity to a grounded probe. These tests were intended to investigate whether small quantities of particulates entrained in a hydrogen release could induce a spark discharge between isolated conductors. The circular copper plate measured 176 mm in diameter and 3.2 mm in thickness. The capacitance of the plate was 360 pF. It was placed in the release at a 45-deg angle relative to the jet’s axis with one of the plate’s flat surfaces facing the nozzle. The grounded probe was a copper rod with a sharp tip on one end that extended to the center of the copper plate. The gap between the circular plate and the grounded probe was 2.5 mm. The available spark energy in each test was calculated using the spark-discharge equation with the voltage measured at the time of ignition and the measured plate capacitance.

In this configuration, six ignitions occurred in eight tests. Ignition occurred in three out of four tests with only 0.1 g of iron (III) oxide particles present. Fig. 6(a) shows the voltage measured on the ungrounded plate for the three tests in which ignition occurred with 0.1 g of iron (III) oxide. On this plot, the ignition time determined using a high-speed video coincided with a voltage spike seen on the ungrounded plate’s voltage measurement. In all cases, ignition occurred when the ungrounded plate reached a voltage between 0.7 and 1.5 kV. These potentials corresponded to available spark-discharge energies between 0.094 and 0.358 mJ. As the flame propagated throughout the jet, the voltage on the ungrounded plate returned to zero and, in some cases, went positive. The return to zero appears to be related to the combustion of the hydrogen jet and not the discharge, as it occurs on both detectors tens of milliseconds after ignition. The drop may be caused by ionization of particulates that occurs during combustion. This ionization may increase conductivity of the gas surrounding the detectors and cause the charge to be conducted away. High-speed video was used to capture the ignition time and location, and the development of the flame for the period just after ignition, to when the flame front propagated to its maximum size. Fig. 6(b) shows selected individual high-speed video frames, referenced to ignition time.

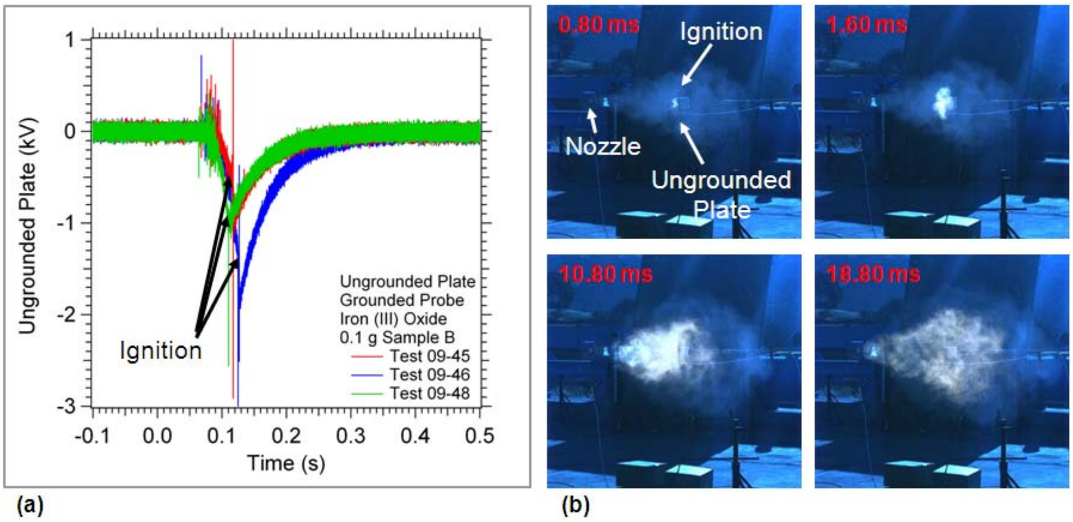

Figure 6. (a) Electrostatic potential measurement on an ungrounded plate with a grounded probe in close proximity for cases with ignition with 0.1 g of iron oxide sample B; (b) High-speed video frames of ignition event referenced to ignition time.

Nozzle Charged-Plate Detector Ignition

The nozzle charged-plate detector was used in a total of 41 tests. In four of these 41 tests, ignition occurred in close proximity to the detector. Two ignition events each occurred with the 76-mm and 127-mm nozzle charged-plate detector. The 76-mm and the 127-mm nozzle charged-plate detectors had capacitances of 180 and 117 nF, respectively. No ignitions occurred when a nozzle charged-plate detector was not present, and no ignitions of this type occurred without particles entrained in the flow.

Fig. 7(a) shows a plot of static charge measurements on the nozzle charged-plate detector for cases with ignition. There is no clear indication of a discrete discharge occurring in these measurements. The discharge mechanism that caused ignition in these tests is unclear and requires further research. In all four cases in which ignition occurred, the nozzle charged-plate detector reached a potential voltage between 2 and 6 kV. The maximum energy stored on the detector varied from 0.41 to 3.20 mJ. As the flame propagated throughout the jet, the voltage on the ungrounded plate returned to zero and, in some cases, went positive. The return to zero appears to be related to the combustion of the hydrogen jet and not the discharge, as it occurs in both detectors tens of milliseconds after ignition. This drop may be caused by ionization of particulates that occurs during combustion.

Fig. 7(b) and Fig. 7(c) show selected individual high-speed and standard video frames from a test in which self-ignition of the hydrogen release occurred in close proximity to the nozzle charged-plate detector. The images show what appears to be the beginning of ignition with a small volume inside the nozzle emitting visible light. In these frames, the flame appears to ignite inside a detector. The light fades and then reappears a few milliseconds later. According to the pressure gage, this event was observed approximately 40 ms after high-pressure hydrogen reached the nozzle. Standard and infrared (IR) video frames show that the iron oxide particulate had already exited the nozzle, and the jet extended between 0.3 and 0.9 m away from the nozzle before ignition occurred. Since ignition occurred near the base of the hydrogen jet, rather than at the leading edge, diffusion ignition does not appear to be the ignition mechanism. At the time of ignition, the pressure just upstream of the nozzle is about 60 bar, while the pressure in the stagnation chamber is about 125 bar. These two pressures begin to track each other at about 140 ms. When the flame reappears in the high-speed video, it propagates away from the detector as a fireball before it begins to propagate back toward the nozzle and throughout the flammable extent of the hydrogen jet.

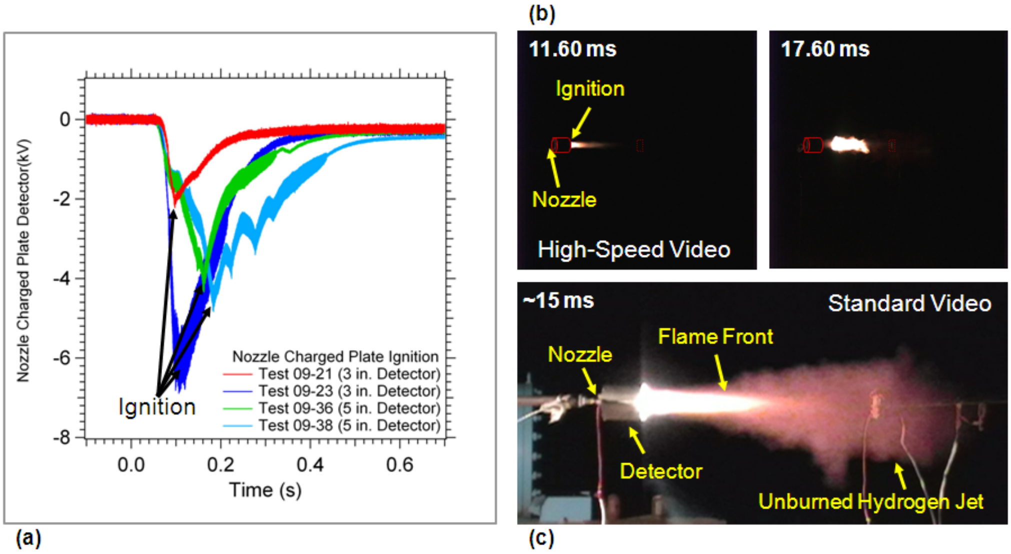

Figure 7. (a) Electrostatic potential on the nozzle charge plate detector for cases with self-ignition; (b) high-speed video; and c) standard video frames of ignition event referenced to ignition time.

Ungrounded Copper Plate Ignition

An ungrounded copper plate was used to investigate the potential for charged particles to cause a spontaneous ignition event by corona discharge. The plate measured 156 mm x 156 mm and was 3.2-mm thick and had a capacitance of 400 pF. The plate was selected because it had sharp tips and a large surface for impact charging, which could lead to the development of a high-strength electric field. The plate was placed in the release at a 45-deg angle relative to the jet's axis; one of the plate's flat surfaces faced the nozzle, and the plate's center was at the attempted ignition location. A total of 13 tests were conducted with the ungrounded plate, and ignition occurred on the plate in two of the tests.

Fig. 8(a) shows the voltage measured on the ungrounded plate in the two tests in which ignition occurred. In both tests, the plate was charged to an electrostatic potential of -13.5 kV at the time of ignition. No distinct discharge was observed at the time of ignition; however, it is possible that a discharge occurred and the Static Level Monitoring System was unable to detect it. Fig. 8(b) shows selected individual high-speed video frames from a test where ignition occurred near the plate. The flame-visualization data show that, in both ignition events, the release was ignited on the edge of the plate. Thus, two ignition mechanisms appear possible, a corona discharge or an electrostatic discharge between isolated conductors. A corona discharge may have occurred when the plate was charged to a high electrostatic potential. However, subsequent tests charged to higher electrostatic potentials (-41.5 kV) repeatedly did not result in ignition. After the second ignition event occurred, it was observed that the plate's charge-monitoring cable had been damaged and that an ungrounded braided wire was in close proximity to the ignition location observed in the high-speed video. A spark discharge between isolated conductors may have occurred if the ungrounded plate and ungrounded cable were charged to significantly different potentials.

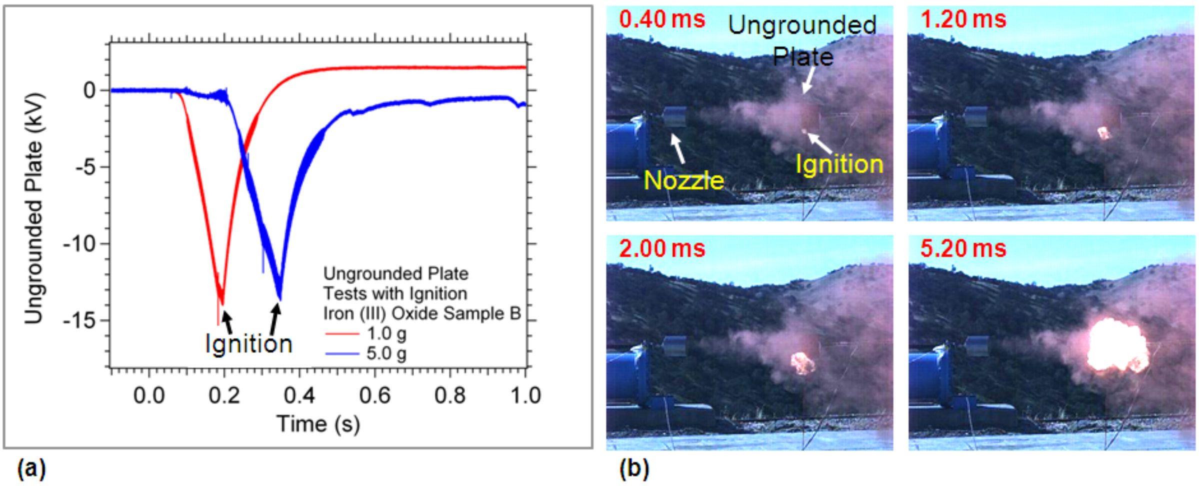

Figure 8. (a) Electrostatic potential measured on the ungrounded plate in tests with ignition; (b) High-speed video frames from referenced to ignition time.

Attempted Ignition Tests in Which No Ignition Occurred

In 10 tests, ungrounded conductors with sharp points were charged to potentials between -12.8 kV and -45.1 kV, and no ignition occurred. The fact that ignition did not occur may be attributed to two factors: (1) The electrostatic potential was not high enough to generate an incendive corona discharge; and (2) the geometry of the plate with a sharp probe was not suitable. Several tests with between 5 – 10 g of iron oxide were conducted, and it is unlikely that increasing the amount of entrained particles would be realistic for a vast majority of hydrogen applications. It is possible that the geometry of the isolated conductor was not suitable to produce an incendive discharge, and the sharp tip allowed the charge to dissipate safely despite it being surrounded by a sensitive hydrogen-air mixture. The results indicate it may be difficult to ignite a hydrogen release with a corona discharge induced by charged particulates. It may be possible using a different geometry, such as a fine wire to create a more severe corona-discharge condition.

It may be more likely for charged particulates in a hydrogen release to induce an incendive brush discharge than an incendive corona discharge. If the isolated conductor's surface were curved in such a way that it had a significant radius of curvature, a brush discharge could have occurred. Brush discharges are more incendive than corona discharges, and at normal atmospheric conditions [23], form between 20 – 25 kV. In four tests, the isolated plate in the release was charged to a negative potential of greater than -20 kV. It is possible that replacing the plate with a suitably shaped conductor (such as a door knob) could lead to ignition by brush discharge. It should be noted that a significant amount of particulates were required to charge the isolated conductor to -20 kV. This indicates that even if a brush discharge induced by entrained iron oxide ignited the release, it is unlikely this would occur from a typical release of this scale. For large-scale releases, it is more likely these quantities of particulates could be present. Future research should be conducted to investigate the self-ignition of a hydrogen release by particulate-induced brush discharge.

4.0 SUMMARY AND CONCLUSIONS

Ignition tests were performed with an external power supply to verify that the release could be ignited at the selected ignition location with a low energy output. One test was conducted with a 110-mJ spark discharge, and ignition occurred. No ignitions occurred when a 15-kV AC corona was placed in the release.

A series of tests with no particles added to the release assessed the charge buildup in a jet produced by the release facility. A substantial amount of charge was generated during the first release, and the charge decreased significantly for subsequent releases. Thus, there is potential for particles present in pressured hydrogen systems, and these particles could generate a significant amount of charge.

Tests were conducted to determine how the charge generated by particulates entrained in the hydrogen release was affected by the type of particle, the mass of the particles, and the particle-entrainment location. Four different iron oxide particle samples were evaluated in external entrainment tests. All four iron oxide samples induced a negative charge on the detector, indicating electrons were stripped from the iron oxide particles, giving them a positive charge. Of the four samples, the iron (III) oxide sample with the largest particles produced the highest charge. The charge increased when particles were entrained inside the system rather than when they were entrained externally. When the mass of particles was varied from 0.0 – 0.5 g, the charge produced increased.

A series of ignition tests was performed with an isolated plate in close proximity to a grounded probe to investigate whether small quantities of particulates entrained in a hydrogen release could induce a spark discharge between isolated conductors. In this configuration, six ignitions occurred with available spark-discharge energies ranging from 0.094 – 0.358 mJ. Ignition occurred in three out of four tests in which as little as 0.1 g of iron (III) oxide particles were present. Thus, even a small quantity of entrained particulates can be a source of spontaneous ignition by electrostatic discharge.

In 4 out of 41 tests performed with an isolated nozzle charged-plate detector, ignition occurred in close proximity to the detector. No ignitions occurred when the nozzle charged-plate detector was not present, and no ignitions of this type occurred without particles entrained in the flow. In all four cases in which ignition occurred, the nozzle charged-plate detector reached a potential voltage between 2 and 6 kV. Standard and IR video frames show that the iron oxide particulates had already exited the nozzle and that the hydrogen jet extended between 0.3 – 0.9 m from the nozzle when ignition occurred. More research is required to determine the cause of these ignitions.

A total of 12 tests were conducted with the ungrounded conductors with sharp points, and ignition occurred in two of the tests. The flame visualization data show that in both ignition events, the release was ignited on the edge of the plate. Two ignition mechanisms appear possible for these tests: an electrostatic discharge and a corona discharge. A spark discharge between the ungrounded plate and an ungrounded cable may have been the source of ignition. All ignition events observed took place in close proximity to ungrounded metal objects. No ignition events were observed in the presence of grounded metal alone. The results indicate the primary concern over electrostatic discharges will be spark discharges between isolated conductors.

The scale of these studies made it difficult to induce an incendive corona discharge by charging an isolated conductor with particulates entrained in the release. In multiple tests, significant quantities of iron oxide particles were entrained, and a sharp-pointed ungrounded conductor was charged to a high potential with no ignition occurring. It is possible that replacing the plate with a rounded conductor could lead to generation of a more incendive brush discharge. However, an incendive brush discharge may also be unlikely to form due to the quantity of particulates required to generate high electrostatic potential. For the scale studied, it is unlikely that a typical hydrogen application will have this quantity of particulate present internally.

ACKNOWLEDGMENTS

This work was supported by the U.S. Department of Energy, Office of Energy Efficiency and Renewable Energy, Hydrogen, Fuel Cells and Infrastructure Technologies Program under the Codes and Standards subprogram element managed by Antonio Ruiz.

REFERENCES

1. Astbury, G.R. and Hawksworth, S.J., Spontaneous Ignition of Hydrogen Leaks: Review of Postulated Mechanisms, *International Journal of Hydrogen Energy*, **32**(13), 2007, pp. 2178–2185.

2. Dryer, F.L., Chaos, M., Zhao, Z., Stein, J.N., Alpert, J.Y. and Homer, C.J., Spontaneous Ignition of Pressurized Releases of Hydrogen and Natural Gas into Air, *Combustion Science and Technology*, **179**(4-6), 2007, pp. 663-694.
3. Mogi, T., Kim, D., Shiina, H. and Horiguchi, S., Self-ignition and Explosion During Discharge of High-Pressure Hydrogen, *Journal of Loss Prevention in the Process Industries*, **21(**2), 2008, pp. 199-204.
4. Wolański, P. and Wójcicki, S., Investigation into the Mechanism of the Diffusion Ignition of a Combustible Gas Flowing into an Oxidising Atmosphere. *14th International Symposium on Combustion*, The Combustion Institute, Pennsylvania State University, 1973, pp. 1217-1223.
5. Groethe, M., Merilo, E., Colton, J., Chiba, S., Sato, Y. and Iwabuchi, H., Large-scale Hydrogen Deflagrations and Detonations, *International Journal of Hydrogen Energy*, **32**(13), 2007, pp. 2125-2133.
6. Reider, R., Otway, H.J. and Knight, H.T., An Unconfined Large Volume Hydrogen/Air Explosion, *Pyrodynamics*, **2**, 1965, 249-261.
7. Anonymous, Spontaneous Ignition of Hydrogen, *Engineering*, **113**, 1922, pp. 502.
8. Fenning, R.W. and Cotton, F.T., Two Unexpected Hydrogen-Air Explosions, *Engineering*, **130**, 1930, pp. 252.
9. Imamura, T., Mogi, T. and Wada, Y., Control of the Ignition Possibility Of Hydrogen By Electrostatic Discharge At A Ventilation Duct Outlet, *International Journal of Hydrogen Energy*, **34**(6), 2009, pp. 2815-2823.
10. Royle, J., Gummer, M., Hooker, P., Willoughby, D. and Udensi, J., Self Ignition of Hydrogen by Various Mechanisms, 18th World Hydrogen Energy Conference, Essen, Germany, 16-21 May, 2010.
11. ISSA, Static Electricity: Ignition Hazards and Protection Measures, 1996, ISSA, Heidelberg, Germany.
12. Hearn, G.L., Static Electricity: Guidance for Plant Engineers, http://www.wolfsonelectrostatics.com/01_hazards/pdfs/guidanceforplantengineers-staticelectricity.pdf
13. Cross, J.A., Electrostatics Principles, Problems and Applications, 1987, Adam Hilger, Bristol, UK.
14. Luttgens, G. and Glor, M., Understanding and Controlling Static Electricity, *Expert Verlag*, 1989.
15. Matsusaka, S. and Masuda, H., Electrostatics of Particles, *Advanced Powder Technology*, **14**(2), 2003, pp. 143-166.
16. Kanazawa, S., Ohkubo, T., Nomoto, Y. and Adachi, T., Electrification of a Pipe Wall During Powder Transport, *Journal of Electrostatics*, **35**(1), 1995, pp. 47-54.
17. Tsochatzidis, N.A. and Maroulis, K., Black Powder Removal From Gas: Evaluation of Methods Based on DEPA’s Experience, 8th International Conference Pipeline Rehabilitation & Maintenance, Istanbul, Turkey, 11-15 September, 2006.
18. NASA. Safety Standard for Hydrogen and Hydrogen Systems: Guidelines for Hydrogen System Design, Materials Selection, Operations, Storage, and Transportation (NSS 1740.16), 1997, Office of Safety and Mission Assurance, Washington, DC.
19. Britton, L.G., Avoiding Static Ignition Hazards in Chemical Operations: A CCPS Concept Book, 1999, American Institute of Chemical Engineers, New York, NY.
20. Glor, M., Ignition Hazard Due to Static Electricity in Particulate Processes, *Powder Technology*, **135–136**, 2003, pp. 223– 233.
21. Ono, R. and Oda, T., Spark Ignition of Hydrogen-Air Mixture, *Journal of Physics: Conference Series*, 2008, **142**, pp. 012003.
22. Schefer, R.W., Merilo, E.G., Groethe, M.A. and Houf, W.G., Experimental Investigation of Hydrogen Jet Fire Mitigation by Barrier Walls, *International Journal of Hydrogen Energy*, **36**(3), 2011, pp. 2530-2537.
23. Britton, L.G. and Smith, J.A., Static Hazards of Drum Filling: II. Electrostatic Models: Theory and Experiment, *Plant/Operations Progress*, **7**(1), 1988, pp. 63-78.